

Direct Coupling of Plasmonic and Photonic Nanowires for Hybrid Nanophotonic Components and Circuits

Xin Guo,[†] Min Qiu,[‡] Jiming Bao,[§] Benjamin J. Wiley,^{||} Qing Yang,[†] Xining Zhang,[†] Yaoguang Ma,[†] Huakang Yu,[†] and Limin Tong^{*†}

State Key Laboratory of Modern Optical Instrumentation, Department of Optical Engineering, Zhejiang University, Hangzhou 310027, China, Lab of Photonics and Microwave Engineering, School of Information and Communication Technology, Royal Institute of Technology, Electrum 229, 16440 Kista, Sweden, Department of Electrical and Computer Engineering, University of Houston, Houston, Texas 77204, and Department of Chemistry, Duke University, Durham, North Carolina 27708

Received September 1, 2009; Revised Manuscript Received October 15, 2009

ABSTRACT

We report direct coupling of plasmonic and photonic nanowires using ultracompact near-field interaction. Photon–plasmon coupling efficiency up to 80% with coupling length down to the 200 nm level is achieved between individual Ag and ZnO nanowires. Hybrid nanophotonic components, including polarization splitters, Mach–Zehnder interferometers, and microring cavities, are fabricated out of coupled Ag and ZnO nanowires. These components offer relatively low loss with subwavelength confinement; a hybrid nanowire microcavity exhibits a Q-factor of 520.

Nanowires are intriguing materials for fundamental studies of light–matter interactions at the nanoscale, as well as for fabrication of nanophotonic components and circuits.^{1–3} Photonic nanowires such as semiconductor nanowires,⁴ glass nanofibers,⁵ and silicon-on-insulator (SOI) waveguides⁶ exhibit low optical loss, but optical confinement in these structures is limited by the diffraction limit (on the order of λ/n , with refractive index n typically less than 5). By coupling light to free electron oscillations in the metal, plasmonic nanostructures provide the possibility to break the diffraction limit and confine light to scales less than $\lambda/10$,^{7,8} as well as to carry optical and electrical signals in the same optoelectronic circuitry.⁹ However, plasmonic nanostructures usually suffer from high losses when light is confined to subwavelength scales, preventing the realization of “all-metal” nanophotonic circuitry. A number of strategies,¹⁰ such as channel plasmon polaritons,¹¹ plasmonic waveguiding with gain medium,^{12,13} and hybrid approaches combining plasmonic with dielectric waveguiding^{14–17} have been suggested to circumvent this problem, but simultaneous realization of

subwavelength confinement and low propagation loss remains a challenge. By substituting low-loss photonic waveguides for metallic counterparts where ultratight confinement is unnecessary, it is possible to fabricate nanophotonic components with relatively low losses, in which the key issue is efficient coupling between the two types of waveguides. In the past years, a variety of approaches for coupling plasmonic and photonic waveguides have been proposed or realized.^{14–19} Compared with the wavelength of the light, the overall size of these structures remains large. Here we demonstrate, for the first time, direct coupling of plasmonic and photonic nanowires via sub-wavelength-scale near-field interaction. Using efficiently coupled plasmonic and photonic nanowires, we further demonstrate the possibility of realizing hybrid nanophotonic components/circuits with subwavelength confinement and reduced loss.

The photonic nanowires used here are silica nanofibers (taper drawn from single-mode fibers⁵) and ZnO nanowires (synthesized via a chemical vapor transport process²⁰), which exhibit low loss (<1 dB/mm) for optical waveguiding.^{4,5} Chemically synthesized Ag nanowires with smooth surfaces are used as plasmon waveguides.²¹ The Ag nanowires were first synthesized and washed using the same methods as have been reported elsewhere,^{21,22} suspended in an aqueous solution, and then deposited on a MgF₂ substrate. When the two types of nanowires are placed close enough, optical near

* To whom correspondence should be addressed, phytong@zju.edu.cn.

[†] State Key Laboratory of Modern Optical Instrumentation, Department of Optical Engineering, Zhejiang University.

[‡] Lab of Photonics and Microwave Engineering, School of Information and Communication Technology, Royal Institute of Technology.

[§] Department of Electrical and Computer Engineering, University of Houston.

^{||} Department of Chemistry, Duke University.

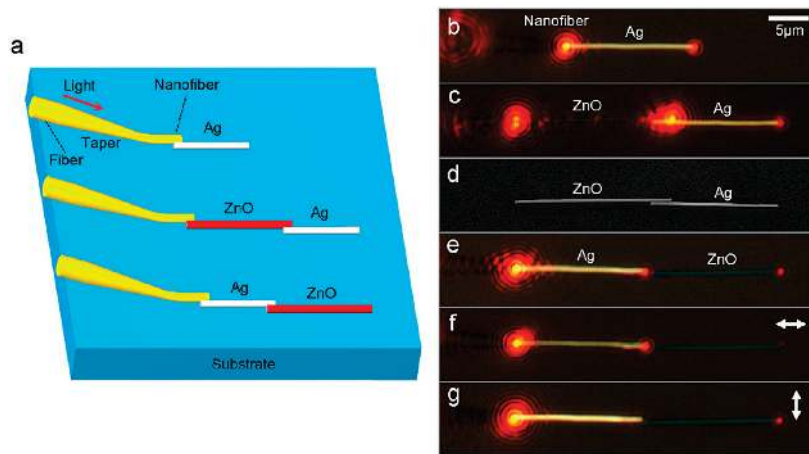


Figure 1. Direct coupling of plasmonic and photonic nanowires. (a) Schematic illustration of light coupling between silica nanofibers (located at distal end of the fiber taper), ZnO nanowires, and Ag nanowires. Light from the nanofiber can excite plasmons in the Ag nanowire directly (top) or via an intervening ZnO nanowire (middle). Plasmons in the Ag nanowire can convert back to light in the ZnO nanowire (bottom). (b, c, e) Experimental observations corresponding to the three different coupling schemes illustrated in (a). (d) SEM image of the coupler shown in (c). The diameter of the ZnO nanowire is 340 nm and the diameter of the Ag nanowire is 320 nm. (f, g) Microscope images taken with the polarization along and perpendicular to the nanowires shown in (e), respectively. Scale bar in (b) applies to (c–g).

field in a sub-wavelength-diameter photonic nanowire and plasmonic near field in a plasmonic nanowire may strongly overlap, resulting in highly efficient photon–plasmon conversion in the coupling area.

Experimentally, light used for excitation was first lens-coupled into a standard fiber (SMF 28, Corning), and then squeezed into the nanofiber through a fiber taper, yielding quasi-circular-polarization guided modes (HE_{11} modes) with high fractional evanescent fields.²³ The waveguiding nanofiber was then brought into contact with ZnO or Ag nanowires by micromanipulation (see Supporting Information). As schematically illustrated in Figure 1a, light from a nanofiber can excite surface plasmons in the Ag nanowire directly (top) or travel through an intervening ZnO nanowire before launching plasmons in the Ag nanowire (middle). Conversely, plasmons in the Ag nanowire can convert back into light guided by the ZnO nanowire (bottom). All the nanowires are supported on a nondissipative substrate for low-loss operation. Figure 1b shows an optical micrograph of 650 nm wavelength light from a nanofiber coupled into a 320 nm diameter Ag nanowire supported on a MgF_2 substrate ($n = 1.38$). With an overlap between the nanofiber and the nanowire of less than $1 \mu m$, light scattered from the output of the $15.7 \mu m$ length Ag nanowire, indicating effective excitation of propagating plasmons in the Ag nanowire. In Figure 1c, the light from the nanofiber coupled into a 340 nm diameter $19.3 \mu m$ length ZnO nanowire, and then effectively excited plasmons in the Ag nanowire, with an overlap of about $2 \mu m$ (see Figure 1d). Figure 1e illustrates coupling of plasmons from the excited Ag nanowire back into guided light in the ZnO nanowire.

Polarization of nanowire outputs in Figure 1e was investigated with a linear polaroid. When the polarization is parallel to the nanowires ($P_{||}$), the output from the Ag nanowire is maximized and the output from the right end of the ZnO nanowire is minimized (see Figure 1f). Conversely,

when the polarization is perpendicular to the nanowires (P_{\perp}), the output from the ZnO nanowire is maximized and the output from the Ag nanowire is minimized (see Figure 1g). This can be explained by the different polarizations of guided modes in the two types of nanowires: the Ag nanowire only accepts $P_{||}$ -polarized modes as guiding modes, while the ZnO nanowire mainly supports P_{\perp} -polarized modes. When light is coupled from the Ag to the ZnO nanowire, the strong near-field interaction enables the efficient transfer: the output of $P_{||}$ -polarized plasmonic modes in the Ag nanowire, which otherwise radiates into free space with polarization perpendicular to the propagation direction at far field, was efficiently picked up by the ZnO nanowire at near field due to the strong mode overlap of the two nanowires and evolved into guiding modes of ZnO nanowire at far field. The high extinction ratio of the nanowire outputs for orthogonal polarizations (over 12 dB) provides an opportunity for nanoscale polarization control.

A hybrid coupler can be readily assembled using a ZnO nanowire and a Ag nanowire, as illustrated in Figure 2a. Such a coupler was experimentally realized with a 270 nm diameter ZnO nanowire and a 240 nm diameter Ag nanowire supported on a MgF_2 substrate, with a coupling length as small as 220 nm (see Figure 2b). The fractional outputs from the Ag nanowire, obtained as the ratio of output intensity of the Ag nanowire to the total output of the both nanowires (see Figure 2c–e), are 4%, 8%, and 64% for 488, 532, and 650 nm light, respectively (see Supporting Information). The higher fractional output of propagating plasmons at longer wavelengths is also verified in Figure 2f, in which a white-light excitation results in red light output from the Ag nanowire. After the guiding losses of the Ag nanowire (about $0.43 \text{ dB}/\mu m$,^{19,24} or 3 dB for the $7.2 \mu m$ length) and the ZnO nanowire (lower than $0.001 \text{ dB}/\mu m$ and therefore negligible) were deducted, the calibrated coupling efficiency from the ZnO nanowire into the Ag nanowire at 650 nm wavelength

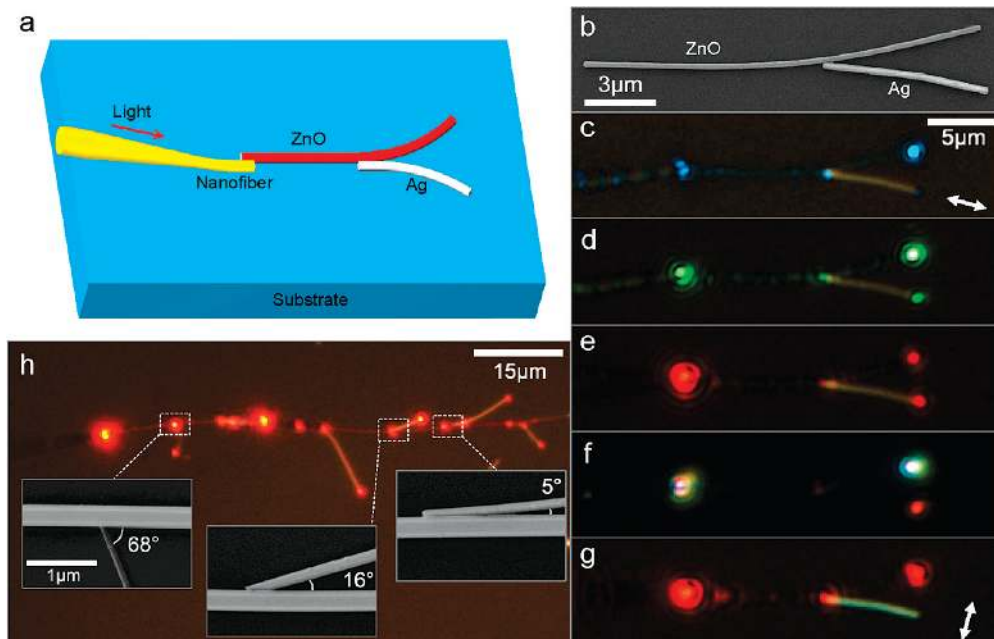


Figure 2. Hybrid couplers fabricated out of coupled Ag and ZnO nanowires. (a) Schematic of a hybrid coupler. (b) SEM image of a hybrid coupler assembled from a 270 nm diameter ZnO nanowire and a 240 nm diameter Ag nanowire. (c–f) Optical micrographs of the hybrid coupler taken with the polarization parallel to the Ag nanowire when monochromatic lasers of wavelength 488, 532, and 650 nm and white light from a halogen lamp are used as light sources. (g) Optical micrograph of the coupler with the 650 nm source when the polarization is perpendicular to the Ag nanowire. Scale bar in (c) is applicable for (d–g). (h) Excitation of multiple Ag nanowires integrated with a single ZnO nanowire. Ag nanowires from left to right are 90, 165, 180, 160, and 115 nm in diameter, with coupling angles ranging from 5° to 68°. Insets, close-up SEM micrographs of typical coupling structures.

(see Figure 2e) is about 82%. Very recently, numerical simulation predicted a coupling efficiency up to 95% when coupling light from a dielectric nanofiber to a metallic nanowire using a butt-coupling scheme,²⁵ indicating higher efficiency is also possible to realize in the side-by-side coupling scheme reported here.

Compared with many other coupling schemes for plasmonic nanowire excitation,^{19,22,24,26} the nanowire-to-nanowire coupling approach offers a much higher efficiency. The high efficiency obtained here benefits from the tightly confined surface modes (evanescent fields) in the ZnO nanowire which, when scattered by the Ag nanowire, create considerable overlap between the incident optical radiation and the propagating plasmon mode. With an orthogonal polarization, output from the Ag nanowire vanishes (see Figure 2g), demonstrating the possibility of operating the hybrid coupler as an ultracompact polarization splitter. Compared with any previous polarization splitter,^{16,27} the hybrid nanowire splitter offers a coupling length 10 times smaller. Figure 2h shows 650 nm light guided along a single 320 nm diameter ZnO nanowire was converted into propagating plasmons in multiple Ag nanowires (insets), representing an ultracompact approach to a recently reported idea for hybrid integration of photonic and plasmonic waveguides.¹⁹

By coupling both ends of a Ag nanowire to a ZnO nanowire (see Figure 3a), we assembled a hybrid Mach–Zehnder interferometer (MZI). Figure 3b shows an optical microscope image of the MZI assembled using a 330 nm diameter ZnO nanowire and a 120 nm diameter Ag nanowire on a MgF₂ crystal, with white light launched in and picked up by fiber tapers (see Supporting Information). The experi-

mentally measured transmission spectrum of the MZI is given in Figure 3c, clearly showing interference fringes with a free space range (FSR) of about 2.75 nm at a wavelength of 710 nm. Theoretically, FSR of the hybrid Mach–Zehnder interferometer is given by

$$\text{FSR} \approx \lambda^2 / (L_{\text{ZnO}} n_{g,\text{ZnO}} - L_{\text{Ag}} n_{g,\text{Ag}})$$

where λ is the wavelength, L_{ZnO} (89 μm) and L_{Ag} (6.5 μm) are the path lengths of the ZnO and Ag nanowires, respectively.²⁸ $n_{g,\text{ZnO}}$ and $n_{g,\text{Ag}}$ are group indices of ZnO and Ag nanowires obtained by $n_g = n - \lambda \text{d}n/\text{d}\lambda$ (n is the index of refraction at wavelength λ). At $\lambda = 710$ nm, for ZnO $n = 1.97$ and $\text{d}n/\text{d}\lambda = -0.18 \mu\text{m}^{-1}$, for Ag $n = n_1 + ik = 0.15 + 4.74i$ and $\text{d}n_1/\text{d}\lambda = 0.044 \mu\text{m}^{-1}$,²⁹ the calculated FSR is about 2.71 nm, which is in good agreement with the experimental measurement.

By use of the complementary ZnO nanowire for optical connection and redirection, the use of the Ag nanowire is minimized, resulting in relatively low insertion loss for the MZI. Due to the favorable waveguiding properties of plasmonic nanowaveguides^{8,30} including tight confinement, field enhancement, and ultrafast nonlinear response, the hybrid nanowire MZI demonstrated here offers great potential for achieving ultracompact functional components and devices ranging from ultrafast optical modulators³⁰ to optical sensors.³¹

Connecting a Ag nanowire with a ZnO nanowire in a closed loop yields a hybrid plasmonic microring cavity. As schematically illustrated in Figure 4a, two additional nanofi-

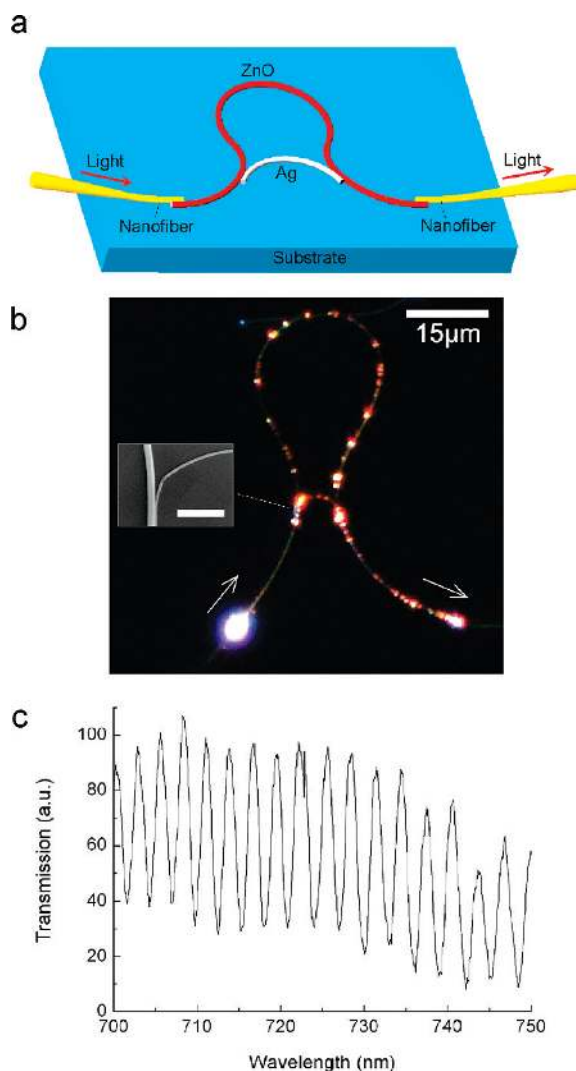


Figure 3. Hybrid Mach-Zehnder interferometer (MZI). (a) Schematic of a hybrid MZI. (b) Optical microscope image of the MZI assembled using a 330 nm diameter ZnO nanowire and a 120 nm diameter Ag nanowire on a MgF₂ crystal, with a white light excitation source. Inset, a SEM image of the coupling area. Scale bar, 2 μm. (c) Transmission spectrum measured with the white light source.

bers and ZnO nanowires were used for optical launching and signal collection with an add-drop technique. Figure 4b shows a SEM micrograph of the hybrid structure assembled with a 400 nm diameter ZnO nanowire and a 265 nm diameter Ag nanowire. The hybrid cavity was characterized by launching a white light at the input port (upper left) and collecting signals from the drop port in the upper right (see inset of Figure 4c). Spectral response given in Figure 4c shows the resonance feature of the cavity, with measured FSR of about 3.8 nm. The FSR of the hybrid microring cavity can be estimated by

$$\text{FSR} \approx \lambda^2 / (L_{\text{ZnO}} n_{g,\text{ZnO}} + L_{\text{Ag}} n_{g,\text{Ag}})$$

where λ is the resonant wavelength.²⁸ $L_{\text{ZnO}} = 99.5 \mu\text{m}$, $L_{\text{Ag}} = 16.5 \mu\text{m}$. At $\lambda = 890 \text{ nm}$, for ZnO $n = 1.95$ and $dn/d\lambda = -0.08 \mu\text{m}^{-1}$, for Ag $n = n_1 + ik = 0.16 + 5.95i$ and $dn_1/d\lambda$

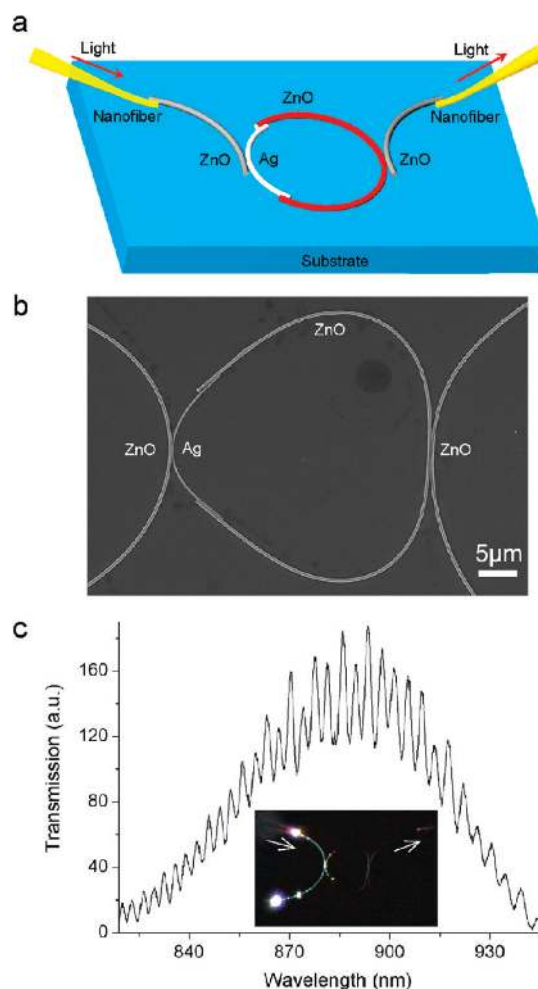


Figure 4. Hybrid microring cavity. (a) Schematic of a hybrid microring cavity. (b) SEM image of a cavity assembled using a 265 nm diameter Ag nanowire and a 400 nm diameter ZnO nanowire in a closed loop. (c) Drop signal of the hybrid cavity characterized with a white light. Inset, dark field optical microscope image of the cavity under investigation.

$= 0.41 \mu\text{m}^{-1}$.²⁹ The calculated FSR is about 4.01 nm, corresponding well to the experimental measurement. The Q -factor of the hybrid cavity, obtained from the full width at half-maximum (fwhm) of the resonant peak around 890 nm, is about 520. Previously reported Ag nanowire cavities of the Fabry-Perot type offer Q -factors less than 100; most light is lost due to the low percentage of light reflected from the ends (about 25%).²⁴ The hybrid structure shown here has similar resistive losses in the Ag nanowire but has greatly improved light recirculation because of the high coupling efficiency (up to 80%) between the ZnO and Ag nanowires and low loss of the ZnO nanowire. The nanowires could be bent to a much smaller radius (on the order of 1 μm),⁴ offering possibilities for making hybrid cavities with much smaller sizes. In addition, the use of high-gain semiconductor nanowires also provides an opportunity for compensating high propagation losses of plasmonic nanowires without sacrificing the tight confinement, enabling fabrication of ultracompact components with low signal attenuation.

The seamless integration of photonic and plasmonic nanowires offers a way to overcome the limitations of

entirely photonic or plasmonic systems and enables the fabrication of nanophotonic components and devices with unprecedented performances. The silica nanofiber input/output scheme utilized here provides a method for connecting nanophotonic/plasmonic circuits with outer fiber communication systems. Also, hybrid nanophotonic/plasmonic systems will enable the fabrication of extremely high densities of optoelectronic devices that exhibit relatively low loss,³² as well lead to useful tools for fundamental research in nanoscale photonics, plasmonics, and quantum optics.^{33,34}

Acknowledgment. This work was supported by the National Basic Research Program of China (No. 2007CB-307003), the National Natural Science Foundation of China (Nos. 60728309 and 10974178), the Swedish Foundation for Strategic Research (SSF), and the Swedish Research Council (VR). Fruitful discussions and experimental assistance from Z. Ma and W. Dai are also gratefully appreciated.

Supporting Information Available: Optical microscope image of a typical fiber taper, assembly processes of hybrid components with ZnO and Ag nanowires, and estimation of fractional outputs and coupling efficiency of the ZnO and Ag nanowires. This material is available free of charge via the Internet at <http://pubs.acs.org>.

References

- (1) Duan, X. F.; Huang, Y.; Cui, Y.; Wang, J. F.; Lieber, C. M. *Nature* **2001**, *409*, 66–69.
- (2) Xia, Y. N.; Yang, P. D.; Sun, Y. G.; Wu, Y. Y.; Mayers, B.; Gates, B.; Yin, Y. D.; Kim, F.; Yan, H. Q. *Adv. Mater.* **2003**, *15*, 353–389.
- (3) Lieber, C. M.; Wang, Z. L. *MRS Bull.* **2007**, *32*, 99–108.
- (4) Law, M.; Sirbully, D. J.; Johnson, J. C.; Goldberger, J.; Saykally, R. J.; Yang, P. D. *Science* **2004**, *305*, 1269–1273.
- (5) Tong, L. M.; Gattass, R. R.; Ashcom, J. B.; He, S. L.; Lou, J. Y.; Shen, M. Y.; Maxwell, I.; Mazur, E. *Nature* **2003**, *426*, 816–819.
- (6) Xia, F. N.; Sekaric, L.; Vlasov, Y. *Nat. Photonics* **2007**, *1*, 65–71.
- (7) Raether, H. R. *Surface Plasmons*; Springer-Verlag: Berlin, 1988.
- (8) Barnes, W. L.; Dereux, A.; Ebbesen, T. W. *Nature* **2003**, *424*, 824–830.
- (9) Ozbay, E. *Science* **2006**, *311*, 189–193.
- (10) Maier, S. A. *Plasmonics: Fundamentals and Applications*; Springer: Berlin, 2007.
- (11) Bozhevolnyi, S. I.; Volkov, V. S.; Devaux, E.; Laluet, J.; Ebbesen, T. W. *Nature* **2006**, *440*, 508–511.
- (12) Nezhad, M. P.; Tetz, K.; Fainman, Y. *Opt. Express* **2004**, *12*, 4072–4079.
- (13) Seidel, J.; Grafström, S.; Eng, L. *Phys. Rev. Lett.* **2005**, *94*, 177401.
- (14) Hochberg, M.; Baehr-Jones, T.; Walker, C.; Scherer, A. *Opt. Express* **2004**, *12*, 5481–5486.
- (15) Steinberger, B.; Hohenau, A.; Ditzbacher, H.; Stepanov, A. L.; Drezet, A.; Aussenegg, F. R.; Leitner, A.; Krenn, J. R. *Appl. Phys. Lett.* **2006**, *88*, 094104.
- (16) Liu, F.; Rao, Y.; Huang, Y. D.; Zhang, W.; Peng, J. D. *Appl. Phys. Lett.* **2007**, *90*, 141101.
- (17) Oulton, R. F.; Sorger, V. J.; Genov, D. A.; Pile, D. F. P.; Zhang, X. *Nat. Photonics* **2008**, *2*, 496–500.
- (18) Maier, S. A.; Friedman, M. D.; Barclay, P. E.; Painter, O. *Appl. Phys. Lett.* **2005**, *86*, 071103.
- (19) Pyayt, A. L.; Wiley, B.; Xia, Y. N.; Chen, A. T.; Dalton, L. *Nat. Nanotechnol.* **2008**, *3*, 660–665.
- (20) Wang, J.; Sha, J.; Yang, Q.; Ma, X. Y.; Zhang, H.; Yu, J.; Yang, D. R. *Mater. Lett.* **2005**, *59*, 2710–2714.
- (21) Wiley, B. J.; Sun, Y. G.; Xia, Y. N. *Langmuir* **2005**, *21*, 8077–8080.
- (22) Sanders, A. W.; Routenberg, D. A.; Wiley, B. J.; Xia, Y. N.; Dufresne, E. R.; Reed, M. A. *Nano Lett.* **2006**, *6*, 1822–1826.
- (23) Tong, L. M.; Lou, J. Y.; Mazur, E. *Opt. Express* **2004**, *12*, 1025–1035.
- (24) Ditzbacher, H.; Hohenau, A.; Wagner, D.; Kreibitz, U.; Rogers, M.; Hofer, F.; Aussenegg, F. R.; Krenn, J. R. *Phys. Rev. Lett.* **2005**, *95*, 257403.
- (25) Chen, X. W.; Sandoghdar, V.; Agio, M. *Nano Lett.* **2009**, *9*, 3756–3761.
- (26) Knight, M. W.; Grady, N. K.; Bardhan, R.; Hao, F.; Nordlander, P.; Halas, N. J. *Nano Lett.* **2007**, *7*, 2346–2350.
- (27) Yang, B. K.; Shin, S. Y.; Zhang, D. M. *IEEE Photon. Technol. Lett.* **2009**, *21*, 432–434.
- (28) Saleh, B. E. A.; Teich, M. C. *Fundamentals of Photonics*; Wiley-Interscience: New York, 1991.
- (29) Palik, E. D. *Handbook of Optical Constants of Solids*; Academic Press: New York, 1998.
- (30) MacDonald, K. F.; Sámson, Z. L.; Stockman, M. I.; Zheludev, N. I. *Nat. Photonics* **2009**, *3*, 55–58.
- (31) Lal, S.; Link, S.; Halas, N. J. *Nat. Photonics* **2007**, *1*, 641–648.
- (32) Li, Y.; Qian, F.; Xiang, J.; Lieber, C. M. *Mater. Today* **2006**, *9*, 18–27.
- (33) Chang, D. E.; Sørensen, A. S.; Hemmer, P. R.; Lukin, M. D. *Phys. Rev. Lett.* **2006**, *97*, 053002.
- (34) Akimov, A. V.; Mukherjee, A.; Yu, C. L.; Chang, D. E.; Zibrov, A. S.; Hemmer, P. R.; Park, H.; Lukin, M. D. *Nature* **2007**, *450*, 402–406.

NL902860D